

RESEARCH ARTICLE

10.1002/2015JA022179

This article is a companion to Santos *et al.* [2016] doi:10.1002/2015JA022146.

Key Points:

- Electrodynamics of equatorial ionospheric plasma bubbles over Brazil during magnetic storms
- Influence of the zonal winds and Hall-to-Pedersen conductivity ratio in the drift of the bubble
- Es layers can be an evidence for the development of the Hall electric field

Correspondence to:

A. M. Santos,
angela.santos@inpe.br;
angelasantos_1@yahoo.com.br

Citation:

Santos, A. M., M. A. Abdu, J. R. Souza, J. H. A. Sobral, I. S. Batista, and C. M. Denardini (2016), Storm time equatorial plasma bubble zonal drift reversal due to disturbance Hall electric field over the Brazilian region, *J. Geophys. Res. Space Physics*, 121, doi:10.1002/2015JA022179.

Received 18 NOV 2015

Accepted 14 MAY 2016

Accepted article online 18 MAY 2016

Storm time equatorial plasma bubble zonal drift reversal due to disturbance Hall electric field over the Brazilian region

A. M. Santos¹, M. A. Abdu^{1,2}, J. R. Souza¹, J. H. A. Sobral¹, I. S. Batista¹, and C. M. Denardini¹

¹National Institute For Space Research, São José dos Campos, Brazil, ²Instituto Tecnológico de Aeronáutica, Departamento de Ciência e Tecnologia Aeroespacial (DCTA), São José dos Campos, Brazil

Abstract The dynamics of equatorial ionospheric plasma bubbles over Brazilian sector during two magnetic storm events are investigated in this work. The observations were made at varying phases of magnetic disturbances when the bubble zonal drift velocity was found to reverse westward from its normally eastward velocity. Calculation of the zonal drift based on a realistic low-latitude ionosphere modeled by the Sheffield University Plasmasphere-Ionosphere Model showed on a quantitative basis a clear competition between vertical Hall electric field and disturbance zonal winds on the variations observed in the zonal velocity of the plasma bubble. The Hall electric field arising from enhanced ratio of field line-integrated conductivities, Σ_H/Σ_P , is most often generated by an increase in the integrated Hall conductivity, arising from enhanced energetic particle precipitation in the South American Magnetic Anomaly region for which evidence is provided from observation of anomalous sporadic *E* layers over Cachoeira Paulista and Fortaleza. Such sporadic *E* layers are also by themselves evidence for the development of the Hall electric field that modifies the zonal drift.

1. Introduction

The effects of vertical Hall electric field in zonal plasma drift of the equatorial ionosphere during magnetic storm disturbances have been studied in recent years [Abdu *et al.*, 1998, 2003, 2012; Fejer and Emmert, 2003; Valentim, 2015; Santos *et al.*, 2016]. Abdu *et al.* [2003] showed that prompt penetration of magnetospheric electric field in the evening equatorial ionosphere can cause post sunset development of plasma bubbles in a season of its quiet time nonoccurrence, and the zonal drift of such bubbles may be reversed to westward from their quiet time eastward drift. This and other studies have shown that while perturbations in the vertical plasma drifts are directly driven by prompt penetration zonal electric field, the zonal plasma drift perturbations can be driven by thermospheric zonal wind perturbation as well as by vertical Hall electric field mapped from the *E* region, where it is produced by the primary zonal penetration electric field under enhanced *E* layer conductivity caused by energetic particle precipitation. In the investigation by Abdu *et al.* [2003] on the development and dynamics of equatorial ionospheric plasma bubble irregularities during an intense magnetospheric storm, it was inferred, on a qualitative basis, that both the prompt penetration electric field as well as disturbance thermospheric winds played key roles in the westward reversal of the zonal drift of the plasma bubble irregularities observed in the course of that magnetic storm. Recently, Santos *et al.* [2016] presented an interesting study on the connection between nighttime ionospheric vertical and zonal plasma drifts measured by the Jicamarca Incoherent Scatter Radar (ISR) during two magnetic storm events. Their objective was to evaluate quantitatively the possible physical parameters responsible for the disturbed zonal drift during epochs of minimum solar activity. It was shown that certain fluctuations in the zonal drift can only be explained if a sufficient increase in the field line-integrated Hall-to-Pedersen conductivity ratio, Σ_H/Σ_P , could occur. This result was based on the calculations performed using a realistic low-latitude ionosphere model simulated by the SUPIM (*Sheffield University Plasmasphere-Ionosphere Model*) in which an enhancement in the *E* region density/conductivity by energetic particle precipitation was included. The model ionosphere so obtained was used in the calculations of vertical electric field/zonal plasma drift.

As mentioned by Abdu *et al.* [2003] and Sobral *et al.* [2011], a westward motion of the ionospheric *F* region at night can be produced in different ways as follows: by quiet time climatological changes in thermospheric zonal winds; by vertical Hall electric field induced by a prompt penetration electric field in the presence of an increase in the *E* region conductivity; by the disturbance dynamo-associated westward thermospheric wind; by disturbance winds during events of high-intensity long-duration continuous *AE* activity (HILDCAA)

that occurs in the absence of geomagnetic storm [Sobral *et al.*, 2006]. However, the conditions for westward motion (instead of the normal eastward motion) can vary depending upon the storm phase. For example, during the November 2004 storm sequences, Li *et al.* [2009] observed, in the Asian longitude sector, westward drift of bubble irregularities on 10 November, in the recovery phase of a severe storm that could be attributed to westward disturbance wind associated with auroral heating. Basu *et al.* [2010] observed in Peruvian longitude sector westward drift of scintillation irregularities on the night of 7–8 November that occurred during the development and recovery phases of an intense storm. The westward drift in this case, we believe, can be attributed to both a disturbance westward wind as well as in part to possible Hall electric field. More recently, a statistical analysis of plasma bubble zonal drift using ion density measurements from the Communication/Navigation Outage Forecasting System satellite by Huang and Roddy [2016] showed that the eastward bubble zonal drift decreased more rapidly with decrease in the *Dst* values, exceeding -60 nT. In this context, this work presents an investigation on the evolution of the plasma bubble zonal velocity that was observed to reverse to westward during the active phases of two storms, one of weak to moderate intensity and the other of severe intensity. The westward reversal in the zonal drift of large-scale plasma depletions (as observed by all-sky optical imagers) was also observed for the smaller-scale irregularity structures diagnosed by a digital ionosonde [Abdu *et al.*, 2003]. The specific objective of the present analysis is to verify and quantitatively evaluate the background ionospheric conditions necessary to cause the bubble zonal velocity reversal (also referred simply as the zonal velocity reversal) to westward (and maintain the westward velocity) during a disturbed period. The analysis is based on a realistic low-latitude ionosphere modeled by the SUPIM- Instituto Nacional de Pesquisas Espaciais (INPE) that is used to calculate all the essential field line-integrated parameters that control the vertical electric field/zonal plasma drift.

2. Experimental Data

The experimental data analyzed here were collected by a 630 nm all-sky imager installed at the INPE optical observatory at São João do Cariri-Brazil (7.4°S , 38.52°W ; magnetic latitude: 8.7°S ; dip angle: -17.2°). The data collected during the magnetic storms of 23–24 September 2003 and 8–9 November 2004 are analyzed in this paper. The zonal plasma bubble velocity was determined from the spatial displacements of the airglow intensity minima in zonal cuts of the all-sky airglow images as described by Sobral *et al.* [2009]. The behavior of the zonal velocity of plasma bubbles was studied together with zonal and vertical plasma drifts of smaller-scale structures (kilometer and decameter sizes) as measured by the Digisonde at Fortaleza (3.9°S , 38.45°W , magnetic latitude: 5.1°S ; dip angle: -10.2°). Modern ionospheric high frequency radio sounders like the Digisonde Portable Sounders can be used to measure the irregularity drifts using the Doppler interferometry technique, the drift being calculated using a software package commonly referred as “Digisonde Drift Analysis” software. This method is implemented by interactive software named Drift Explorer, which allows the determination of the three components of the plasma drift, V_N , V_E , and V_z (north, east, and vertical components). For more details about the drift velocity calculations by the Digisonde, see Reinisch *et al.* [1998], Kozlov and Paznukhov [2008], and Kouba *et al.* [2008]. The daytime vertical drift calculated from the magnetic field variation (ΔH) at São Luis (2.33°S , 44.6°W ; dip angle: -1.6°) and Vassouras (22.4°S , 43.7°W ; dip angle: -34°)-Brazil will also be analyzed. The methodology used in this calculation is as described by Anderson *et al.* [2002]. Sporadic *E* layer signatures in the Digisonde ionograms are also used in this study. The analysis is also supported with the use of magnetic activity indices (interplanetary magnetic field (IMF) B_z , auroral activity *AE*, Sym-H/*Dst*) and the thermospheric zonal wind as per the horizontal wind model (HWM). The electrodynamic process responsible for the plasma bubble drift reversal to westward is evaluated using a realistic low-latitude ionosphere model simulated by the SUPIM that was modified extending its lower height limit to 90 km (from the original 120 km limit). We denote this model as SUPIM-INPE. An extraionization density in the *E* region was added to the SUPIM-INPE to examine/evaluate the effect of energetic particle precipitation in the South American Magnetic Anomaly (SAMA) on the generation of the Hall electric field capable of controlling the zonal plasma drift (for more details about this extraionization in SUPIM-INPE model, see Santos *et al.* [2016]).

3. Results and Discussion

3.1. The Magnetic Storm of 23–24 September 2003

The interplanetary and geomagnetic indices during the days from 21 to 24 September 2003 are presented in Figure 1. The oscillatory behavior, the long durations, and the moderate/strong intensity of these indices

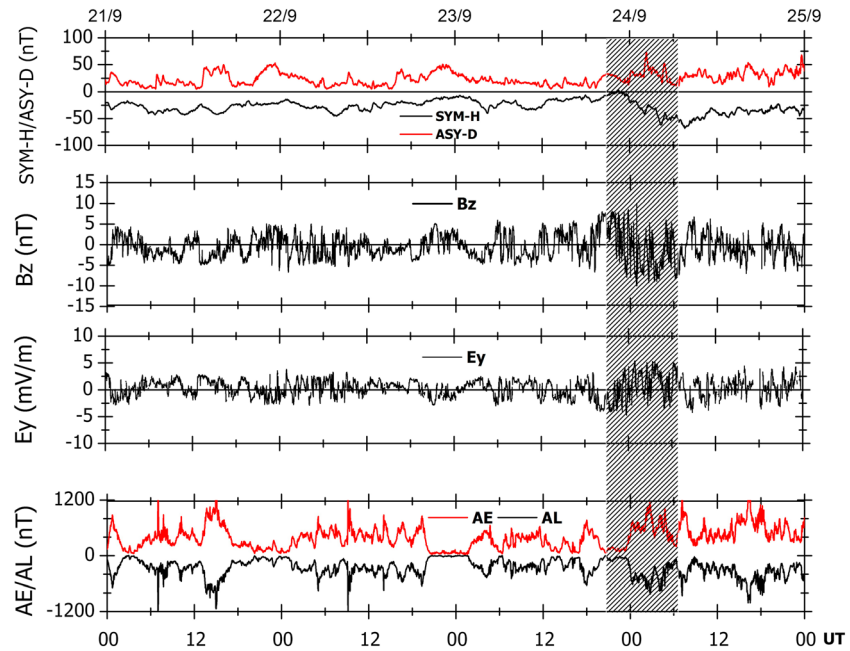


Figure 1. Variation in magnetic indices during the period of 21 to 24 September 2003. (first panel) The Sym-H/Asy-D, (second panel) the IMF- B_z from ACE satellite, (third panel) the electric field E_y , and (fourth panel) the AE/AL indexes. Important fluctuations in vertical and zonal plasma drifts were observed in the interval denoted by the shaded area and will be discussed in the text.

might indicate that the electrodynamics responsible for the plasma bubble westward motion during the nights of 23–24 September could have had significant contributions from effects originating from penetration electric field and energetic particle precipitation and possible effects from disturbance zonal wind and dynamo electric field, as we shall examine below. We may note that during the interval in which the storm-associated zonal drift modification was observed (on the nights of 23–24 September highlighted by the shaded area in Figure 1), the Sym-H/ Dst index attained a minimum value of ~ -60 nT, the interplanetary magnetic field (B_z) oscillated between -10 nT and 10 nT, and the interplanetary electric field E_y showed rapid variations between -5 and 5 mV/m, and the auroral activity (AE) index fluctuated attaining peak values higher than 1000 nT.

Figure 2 shows the B_z and AE indices (Figures 2a and 2b), the zonal drift of the plasma bubble as observed by an all-sky 630 nm optical imager over São João do Cariri (Figure 2c), the vertical (V_{z_DE}) and zonal (V_{y_DE}) velocities of the smaller-scale structures as observed by a digital ionosonde at Fortaleza (Figures 2d and 2e) (where DE indicates that the drift velocities were calculated by the Digisonde Drift Explorer software) and also the blanketing frequency of sporadic E layer ($f_b E_s$) from the same location (Figure 2f). The gray curve in Figure 2c represents the quiet time mean plasma bubble zonal drift (calculated as the mean of the days 26 and 30 September; 23 and 25–27 October; 19, 24, and 26 November; 19–20 December 2003). The dotted blue lines in Figures 2c and 2e are used to indicate the dominant variation trends in respective parameters. We may note a good degree of agreement, for a considerable duration after $\sim 21:00$ LT, between the variations of the zonal drift of plasma bubble as measured by the optical imager and that of the plasma irregularities sampled by the Digisonde (Figures 2c and 2e) and also a clear anticorrelation (in most part) between vertical and zonal plasma drifts (Figures 2d and 2e).

In Figure 2a, we may observe that the interplanetary magnetic field B_z turned to south at $\sim 23:10$ UT (as indicated by a red arrow) which was soon followed by auroral activity intensification (Figure 2b). Although B_z turned northward at 23:40 UT, it reverted to south at 00:30 UT with AE activity maintaining its intensity. From 00:30 UT (21:30 LT) onward, we may note that the downward V_{z_DE} (Figure 2d) started to decrease, indicating an evolving upward drift, which was present till about 03:00 LT (06:00 UT) well after its reversal to upward that had occurred at $\sim 00:00$ LT (03:00 UT). Also, after the upward reversal the vertical drift fluctuated with small amplitude till around 03:00 LT (06:00 UT). This behavior in the vertical drift appears to result

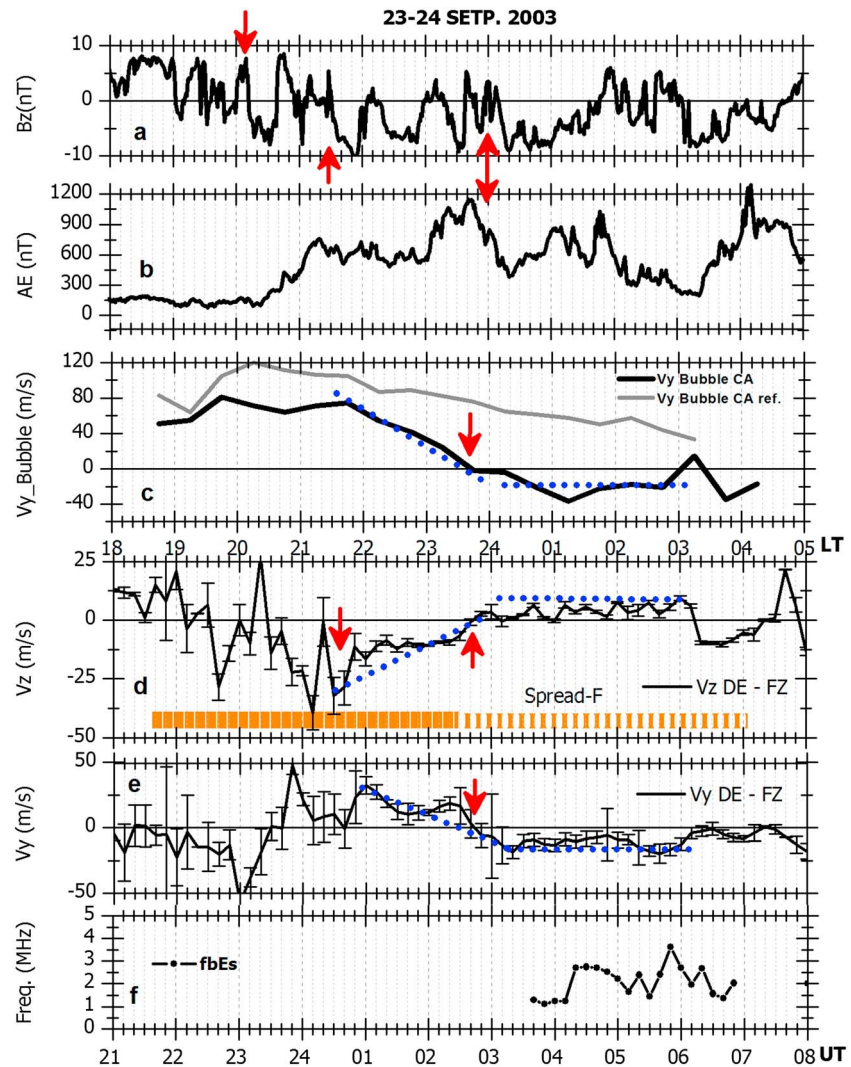


Figure 2. (a) The B_z and (b) AE variations during 23 and 24 September 2003. (c) The plasma bubble zonal drift velocity over São João do Cariri (black curve), wherein the gray curve represents the quiet day mean. (d) The vertical and (e) zonal plasma drifts and (f) the blanketing frequency of Es layer obtained from the Digisonde operated at Fortaleza. The horizontal orange bar indicates the occurrence of spread F, and the dotted blue lines indicate the presence of a good correlation between the zonal and vertical drifts. The red arrows denote some important features that will be discussed in the text. The error bars in the drift measurement by the Digisonde Drift Explorer (DE) at each vertical and zonal plasma drift velocity are also shown in Figures 2d and 2e.

from a long duration imperfectly shielded penetration electric field, marked by alternating presence of undershielding and overshielding conditions, associated with the continuing long duration (and fluctuating) AE activity under a fluctuating and dominantly southward B_z [see for example, Richmond *et al.*, 2003; Huang *et al.*, 2007]. Although it is very difficult to make a clear identification of the minor scale response features in the vertical drift variation in the presence of the long-duration disturbances, some of the specific features do appear to be identifiable. For example, the B_z turning north at 23:40 LT (02:40 UT) followed by a rapid decrease in AE (indicated by a red arrows) appears to have produced an overshielding electric field of eastward polarity that seems to have contributed to the V_z turning positive near 00:00 LT (03:00 UT). In this connection, it is worth pointing out that overshielding electric field associated with rapid decrease in AE activity (during periods of extended AE activity) has been reported before by Abdu *et al.* [2009] in whose case the overshielding electric field was observed at an earlier local time (21:00 LT) when its polarity was westward as expected, however. The V_z continued upward with small fluctuation till ~03:00 LT (06:00 UT). Also, as mentioned above, such fluctuations in the V_z might suggest the presence of corresponding fluctuations in the

penetration electric field arising from the fluctuating nature of the B_z and AE activities. The presence of a smoothly varying disturbance dynamo electric field (DDEF) with eastward polarity may also be considered at these hours, although it is unlikely in this case since the bubble development occurred during the growth phase of a relatively weak storm (see Figure 1) with the minimum Dst of around -60 nT only. Then, at 03:05 LT (06:05 UT), with the B_z rapid southward turning, followed by AE intensification, an undershielding penetration electric field of westward polarity caused a rapid downward motion of the vertical drift over Fortaleza clearly seen at \sim 03:10 LT (06:10 UT) in Figure 2d. This downward vertical drift lasted till \sim 04:30 LT. We may note that the V_z reversal to upward at 23:40 LT (02:40 UT) coincided exactly with the zonal drift reversal to westward, in the Digisonde data plotted in Figure 2e, which agreed with the optical imager data plotted in Figure 2c as indicated by the red arrows. We believe that this zonal drift reversal was caused by the development of a vertical (upward) Hall electric field that was induced by the primary zonal penetration eastward electric field responsible for the simultaneous V_z reversal to upward. The zonal drift pattern of the plasma bubbles from the optical imager (Figure 2c) and that of the smaller irregularities from the Digisonde measurement (Figure 2e) do appear similar starting from \sim 22:00 LT (01:00 UT) till nearly the end of the data. We need to point out that the irregular nature of the V_z and V_y , before 21:30 LT (00:30 UT) may have to do with the severity of the spread F echoes whose presence is indicated by the orange broken lines shown in Figure 2d. We may observe that the zonal drift of the plasma bubble during this day was very different from that of average quiet days (gray curve, Figure 2c). The quiet day drift is of larger velocity and is always eastward during the entire local time period shown here (till 03:00 LT), the drift value decreasing slowly from 120 m/s at \sim 20:30 LT to \sim 40 m/s at 03:00 LT.

Due to the long-duration auroral activity identified in the period before the beginning of the zonal drift variations (as shown in Figure 1), we may expect the variations in the drift to have contribution also from direct and indirect effects of disturbance winds originating from auroral heating. The direct effect may arise from any disturbance zonal wind driving the zonal plasma drift through generation of polarization electric field. Such a situation is possible in view of the auroral activity sequence (Figure 1) that prevailed during the days that just preceded the equatorial observations, although the AE activity was quiet for a few hours prior to drift variations (as evident from Figure 2). The indirect effect may arise from the electric field created by the disturbance dynamo electric field (mentioned earlier) that has its generation at geomagnetic latitudes of $\sim 45^\circ$ but extending nearly instantly to the equatorial region through the Pedersen electric current [Blanc and Richmond, 1980]. It is interesting to note in Figure 1 that during all the time before the period in which the bubble was moving to west, the auroral activity was detected in the absence of a significant magnetic storm, but with B_z oscillating rapidly around zero. This oscillatory behavior characterizes this event as a HILDCAA (high-intensity long-duration continuous AE activity), during which energetic particle injection to auroral region can occur leading to heating and development of disturbed winds (for more details on the HILDCAA phenomenon, see Tsurutani and Gonzalez [1987] and Sobral *et al.* [2006]). However, there are no measurements of disturbed winds to evaluate this hypothesis, and its contribution to the westward reversal (near midnight) of the bubble irregularity drift is found to be insignificant, as we shall discuss later.

Below we will show from model calculations that the connection between zonal and vertical plasma drifts as observed here is possible through development of vertical Hall electric field that can be induced by the primary penetration zonal electric field in the presence of enhanced conductivity in the E region due to energetic particle precipitation, associated with the storm. Furthermore, as shown by Abdu *et al.* [2013], this same Hall electric field can also control the formation of the sporadic E layers. In this context, we note that sporadic E layers were observed over Fortaleza, as indicated by the $f_b E_s$ parameter (Figure 2f) during the general period when the plasma bubble and associated irregularities drifted westward (from \sim 03:00 UT). The formation of such sporadic E layer provides strong indication of an increase in the E region ionization, as will be discussed later.

3.1.1. Model Results

The zonal drift was calculated using a realistic low-latitude ionosphere simulated by the SUPIM-INPE. The details of the model and the procedure used to calculate the key parameters (using field line-integrated quantities) that control the zonal plasma drift were given in Santos *et al.* [2016]. Therefore, they will not be repeated here.

Figure 3 presents in different panels the key parameters used in the calculations and the results obtained under different conditions of the ionosphere as described below. Figure 3a shows the auroral activity (AE) index variation during the period. The ratio between field line-integrated Hall and Pedersen conductivities

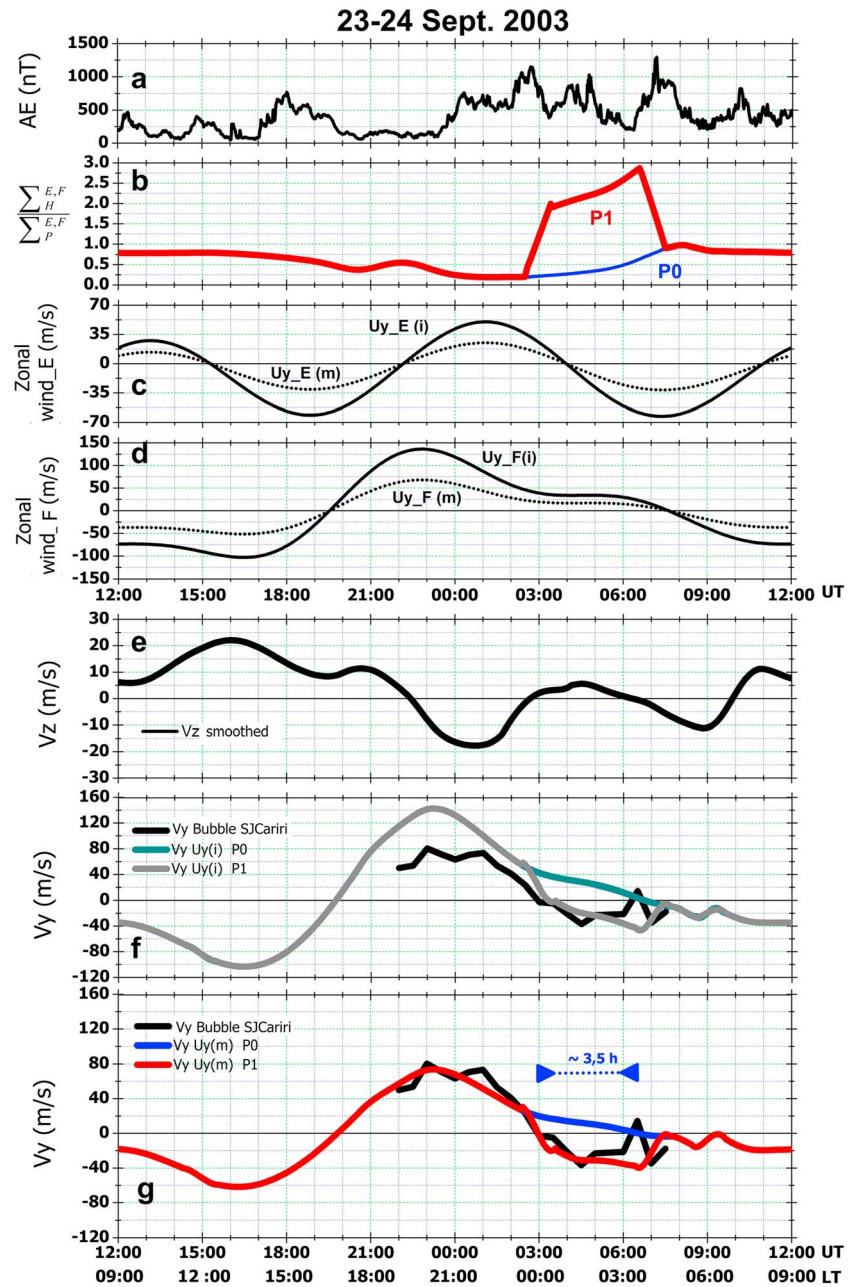


Figure 3. (a) The auroral activity, (b) the ratio Σ_H/Σ_P considering (P1)/not considering (P0) the effects of energetic particle precipitation, the initial U_y (i) and modified U_y (m) zonal wind of the regions (c) E and (d) F, (e) the vertical drift V_z , (f) the observed (black line) and calculated zonal drift considering the initial winds and the inclusion (gray line)/not inclusion (green line) of the precipitation, and (g) the calculated zonal drift considering a correction in the wind and the inclusion/not inclusion of the precipitation. The black curve in Figure 3g is the observed bubble zonal drift.

considering (P1) and not considering (P0) an extraionization in the E region is shown in Figure 3b. Figures 3c and 3d show the initial and modified zonal winds of the E and F regions, and Figure 3e shows the smoothed vertical drift (obtained from the adjacent averaging method) over Fortaleza as deduced from magnetometer data during the day and from Digisonde data during the night. The observed zonal drift of plasma bubble (black curve) is plotted together with the calculated zonal drifts (gray and green curves in Figure 3f). The zonal drift calculated considering an extraionization in the E region by energetic particle precipitation, denoted by P1, is represented by the gray curve, while the drift without such extraionization (denoted by P0) is represented by the green curve. The comparison between the calculated (gray and green curves)

and observed (black curve) zonal drifts shows clearly that although some differences can be identified between them, mainly around 23:00 UT; a better agreement is obtained during the period of 03:00–07:00 UT only if an extraionization by the particle precipitation is included in the calculations, which corresponds to a two-step increase in the ratio Σ_H/Σ_P from 0.25 to 2 and then from 2 to 2.7 as shown by the red curve Figure 3b. We may note that the rise in this ratio was needed to be maintained until ~06:40 UT to make sure that the bubble drift progressed clearly westward. Furthermore, it is important to note that the westward reversal of the drift at 03:00 UT could be simulated only in the case in which the particle precipitation was included.

The results shown in Figure 3f call our attention to two additional features: (1) the calculated drift velocity, at its peak near 23:00 UT, was ~140 m/s, while the observed drift velocity of the bubble was ~80 m/s around that time and (2) the time of the calculated zonal velocity reversal (to west) was slightly delayed in relation to the observed bubble velocity reversal time. Although the particle precipitation has been fundamental to obtain a better matching between the observed and calculated drift variations, the disparity between the drift reversal times and the large difference (of ~60 m/s) between the observed and calculated drifts around 23:00 UT would suggest that additional factors are needed to be considered for finding an agreement between the two results. Part of the differences can be thought to be the height differences involved in the measured wind and the modeled wind used in the calculation. The optical (630 nm airglow) technique generally refers to an altitude of about one scale height below the F layer peak height, while the reference altitude of the model wind can be a bit higher. In this work we consider equivalency in the altitudes of bubble drift velocity and that of the model neutral wind as well as equivalency between the velocity of the plasma bubble and that of the background plasma drift [see Sobral *et al.*, 2011].

As a useful reference for our analysis, we evaluated the characteristics of the plasma zonal drifts over Jicamarca (from ISR measurements) and assumed that they should be closely similar to those over the Brazilian equatorial sector (São João do Cariri). In a separate analysis (not shown here), we found that the zonal drift over Jicamarca for some days (22, 23, 24, 25, and 26) of September 2003 presented maximum values of the daytime westward plasma drift at ~60 m/s, while the evening peak (around 21:00 LT) in eastward plasma drift varied around ~100 m/s. In comparison to these values, our calculated zonal drift in Figure 3f shows the peak westward drift to be near 100 m/s and the peak eastward plasma drift at ~140 m/s. This analysis would suggest that the wind model used in our calculations can be modified to achieve consistency between the modeled drifts and their observational values. Although Jicamarca is situated at a longitude of small eastward magnetic declination angle (~4°E), whereas the Brazilian observatories are located at a large westward declination (~21°W), the criterion used to modify the zonal wind over Brazil based on the zonal drift characteristic over Jicamarca is well justified due to the fact that the zonal plasma drift and zonal wind velocities can be considered to be approximately equivalent. Thus, the zonal wind model (HWM93) used in our calculation of the zonal drift was suitably adjusted to obtain satisfactory results on zonal drift variations. Thus, it was found necessary to multiply the HWM93 zonal wind by a factor of 0.5.

In Figure 3g, the blue curve shows the drift variation obtained considering only the modifications in the zonal wind magnitudes and the red curve is the result obtained by modifying the zonal wind as well as by including the effects of the energetic particle precipitation. The initial (i) and modified (m) winds of the E and F regions are shown in Figures 3c and 3d. As indicated by the blue curve in Figure 3g, the correction in the zonal wind (dotted curves in Figure 3c–Figure 3d) was very important during the nighttime between 19:00 LT and 23:30 LT, when the (observed) eastward velocity was smaller than the initially calculated drift velocity. But this is not so regarding the time of the drift reversal to westward (at ~03:00 UT) and during the interval in which the bubble maintained its westward movement. When only the modification in the winds was considered, the westward reversal of the drift occurred 3.5 h later than in the observational data. On the other hand, the red curve shows that when the effects of particle precipitation is also taken into account, a good agreement between calculated and observed drifts can be found, both regarding the drift reversal time as well as during the period of westward drift that followed. In Figure 3b we may note that it was necessary to increase the ratio Σ_H/E_p from 0.25 to 2 to cause the total reversal of the plasma bubble to westward and then the ratio was increased from 2 to 2.5 (during 4 h) in order to maintain the bubble westward displacement. The increase in this ratio was the result of a considerable relative increase in the field line-integrated conductivities. The degree of increase in the Hall conductivity being significantly higher than that in Pedersen conductivity was produced by enhanced ionization in the E region due to an energetic electron flux varying between

1.1×10^6 electrons $\text{cm}^{-2}\text{s}^{-1}$ and 2.9×10^5 electrons $\text{cm}^{-2}\text{s}^{-1}$, in the energy range from 2 to 32 keV based on measurements by Discover 29 satellites in a passage over SAMA [see also Santos *et al.*, 2016].

3.1.2. Increase in the Nighttime E Region Ionization Detected by the Digisondes

Evidences of an increase in the E region ionization during this magnetic storm was obtained from the Digisondes operated both at Fortaleza (FZ) and at Cachoeira Paulista (CP) that are located in a region strongly affected by the energetic particle precipitation due to the SAMA [Abdu *et al.*, 2005]. It has been shown in previous studies [e.g., Abdu *et al.*, 2013] that the occurrence of sporadic E layers with certain distinct characteristics is a clear manifestation of additional ionization due to energetic particle precipitation in the E region in the SAMA region under magnetic storm disturbances. The sequential ionograms over FZ presented in Figure 4 and those over CP presented in Figure 5 together provide evidence of extraionization in the night E region due to energetic particle precipitation. It may be pointed that the CP station is situated closer to the central region of the SAMA. In order to verify the influence of field line-integrated conductivities on the equatorial F region plasma zonal drift, we need to examine the Es layer development at a low-latitude regions that is field line mapped to equatorial apex height where plasma zonal drift is measured. The Es layer presence that can influence the F region zonal drift over Fortaleza should therefore be sought at a latitude a few degrees northward of CP. An examination of the ionograms in Figures 4 and 5 shows that sporadic E layer formation started first over Cachoeira Paulista (in the ionogram at 23:45 UT) and later over Fortaleza (in the ionogram at 03:00 UT). On this basis, it is reasonable to assume that the Es layer formation at the appropriate latitude (northward of CP) should have started in between their starting times at CP and FZ. The characteristics of the Es layer traces, such as the range spreading and the blanketing of the F layer traces, as well as the group delay effect at the lower frequency end of the F layer trace (seen in some ionograms) as observed over both locations (for example, in the ionograms at 04:00 UT, 04:30 UT, 05:00 UT over Fortaleza and at 00:45 UT, 04:30 UT, 05:00 UT, etc. over CP) are strong indications of the presence of night E layer ionization by energetic particle precipitation [see, for example, Abdu *et al.*, 2013]. The Es layer activity lasted till 06:30 UT over CP and continued till after 07:20 UT over Fortaleza. It is important to note that the B_z was generally southward (with some short duration of northward excursions) during this period of Es activity which also coincided with the bubble zonal drift westward reversal at 03:00 UT and the continuing westward drift till at least 07:30 UT (black curve in Figures 3f and 3g). These results therefore strongly support the understanding that zonal plasma bubble drift during this event sequence was controlled significantly by vertical Hall electric field that was induced by disturbance zonal electric field in the presence of enhanced conductivity in the E region produced by energetic particle precipitation in the SAMA region.

We need to point out in this context that the Es layer evolution pattern at both locations (CP and FZ) involved complex processes due to the possible role of neutral wind dynamics and the different magnetic inclination angles that control their development at the two locations. At Fortaleza, the Es first appeared at ~ 160 km in the ionogram at 03:50 UT, and in subsequent ionograms, the height ($h'Es$) decreased, that is, the layer descended in a way compatible with the descent of the wind shear null point in the downward phase propagation of a tidal mode responsible for the production of the Es layer by wind shear mechanism [Whitehead, 1970; Mathews, 1998]. The layer descended to 100 km as can be noted in the ionogram at 07:20 UT. In the course of the descent, the layer intensified as indicated by the f_bE_s (for example, in the ionograms at 04:20 to 06:00 UT) and evolved with large increase in the range spreading echos (ionogram at 07:20 UT), which has been shown to be a manifestation of irregularities formed at the topside/negative gradient region of an Es layer formed under disturbed conditions [Abdu *et al.*, 2013]. Over CP, on the other hand, the Es layer trace present in the ionograms was weak until 00:15 UT, and what appears to be the disturbance-associated Es layer began at 00:45 UT and evolved with fluctuating intensity and strong range spreading echoes until 06:30 UT. It is important to observe that this Es layer was not of descending type, the height remaining always near 105 km, which is again compatible with the characteristics identified for the Es layer formed due to energetic particle precipitation in the SAMA region [Abdu *et al.*, 2013].

3.2. The Magnetic Storm of 8–9 November 2004

The same methodology employed in the earlier case was used to study the impacts of the magnetic storm on the plasma bubble zonal drift reversal to westward observed on the night of 8–9 November 2004. Figure 6 (top to bottom) shows the geomagnetic indices (SYM-H/ASY-D), the interplanetary magnetic field component (B_z), the corresponding interplanetary electric field (IEF E_y), and the auroral activity indices AE/AL for a

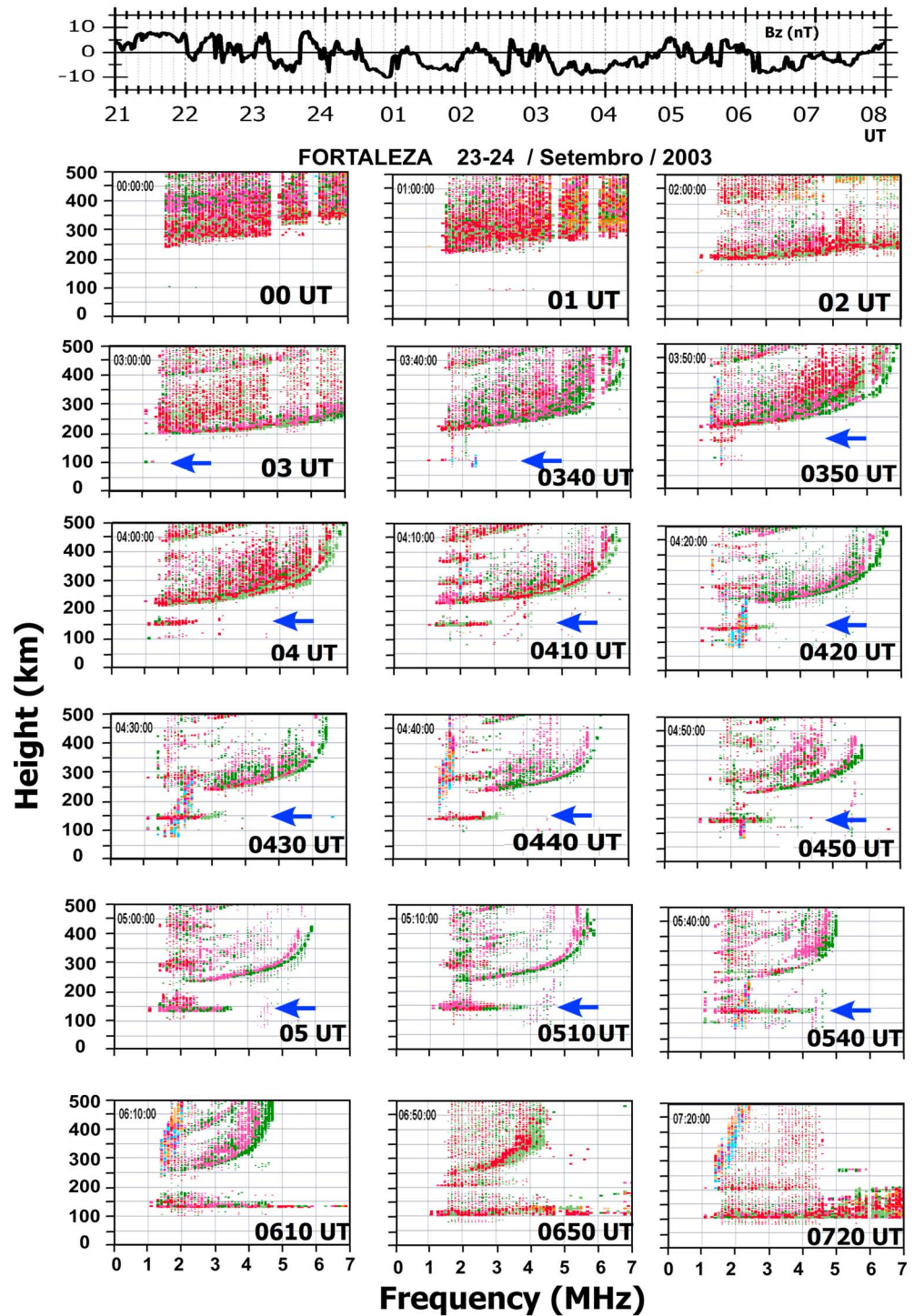


Figure 4. Ionograms from Fortaleza during 23 and 24 September 2003. The blue arrows indicate the presence of *Es* layers. (top) The behavior of the interplanetary magnetic field.

4 day interval surrounding the 8–9 November storm. Typical quiet day behavior can be seen to prevail until 12:00 UT on 7 November. Soon after this time, the storm disturbances started with weak fluctuations in the magnetic indices that soon intensified with the B_z turning south at $\sim 19:00$ UT accompanied by the storm development with the $Dst/SYM-H$ attaining -400 nT that characterizes this as a severe storm event. The large southward increase in the B_z (eastward IEF), with the accompanying large *AE/AL* intensification that started at

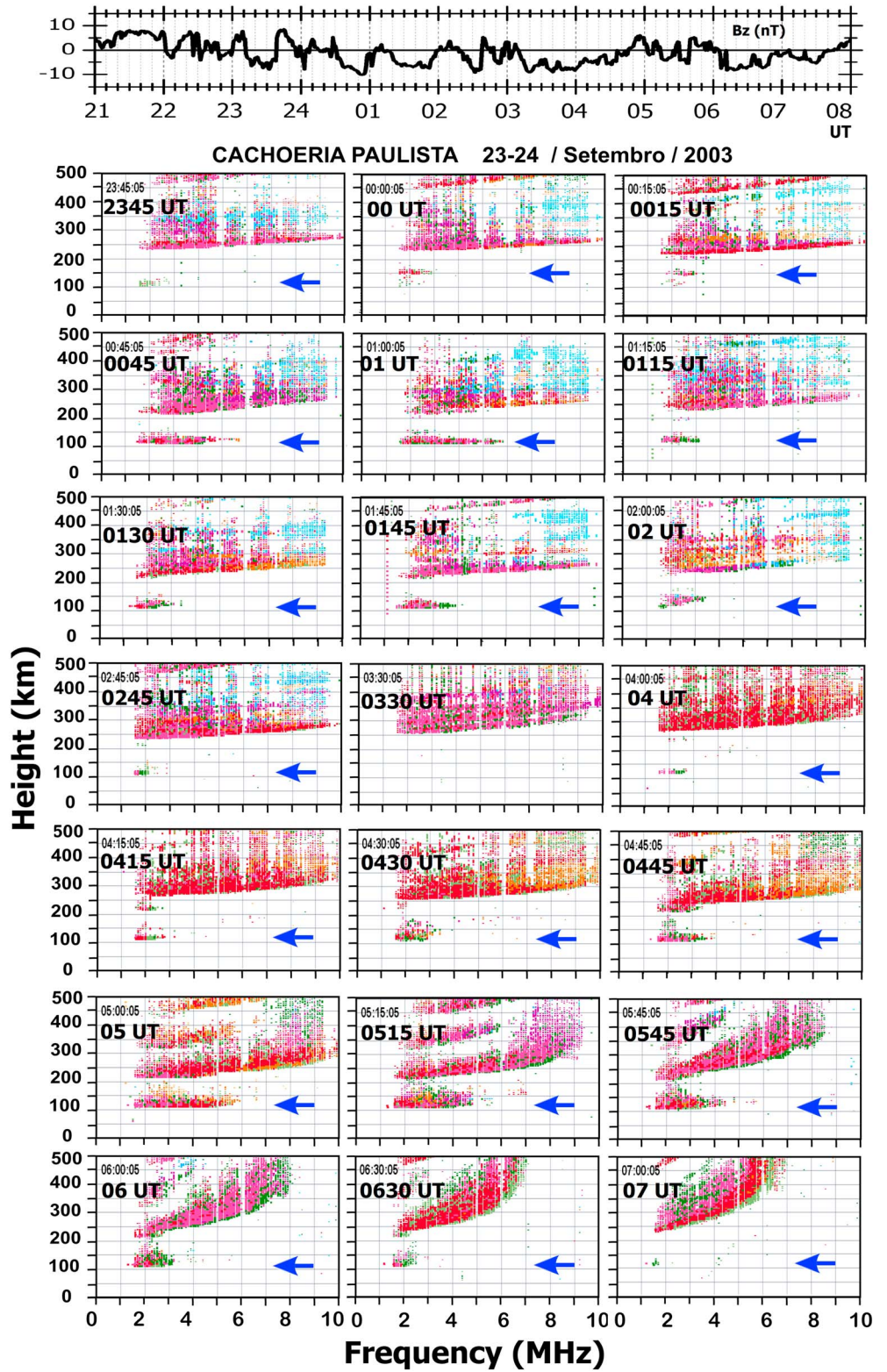


Figure 5. Similar to Figure 4 but for Cachoeira Paulista.

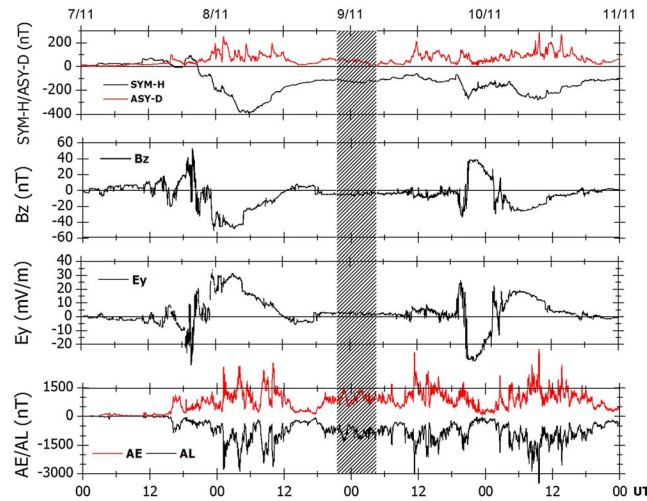


Figure 6. Similar to Figure 1 but for 5–10 November 2004.

(Figure 7c), the vertical (Figure 7d) and zonal (Figure 7e) plasma drift over Fortaleza as measured by the Digisonde, and the sporadic *E* layer blanketing frequency, $f_b E_s$, over Fortaleza (Figure 7f). We may note in panels Figures 7a and 7b that the *AE* activity presented rapid variations under the B_z south condition during the entire period, which might suggest the presence of penetration electric field with interspersed under-shielding and overshielding transients. We may note in particular that the auroral activity intensified from 23:30 UT to 02:00 UT, the *AE* index increasing from ~600 nT to ~1500 nT during this period. The plasma bubble zonal velocity that was eastward, but notably weaker than its quiet time values (gray curve in Figure 7c), reversed to westward at 00:40 UT (21:40 LT) and remained westward till the end of the data at 05:00 UT (02:00 LT). In this case, the zonal plasma bubble velocity of 6 November was used to represent the quiet time drift.

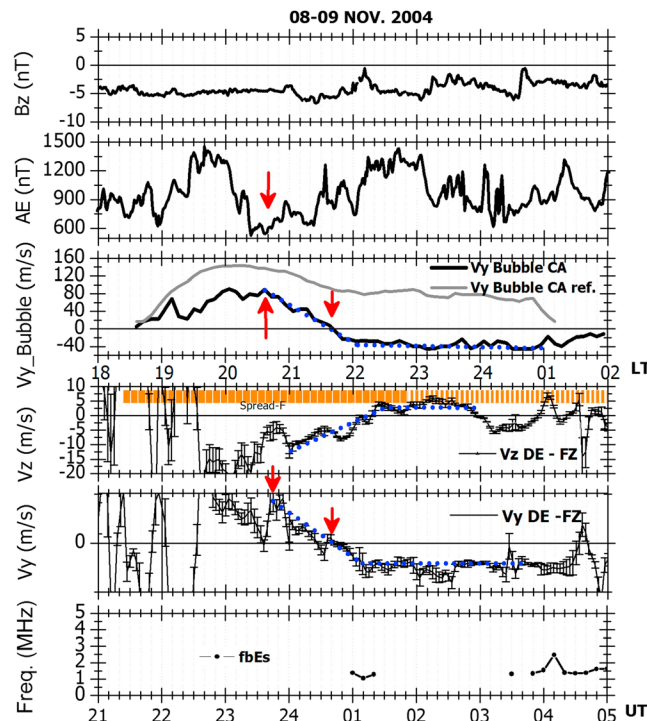


Figure 7. Similar to Figure 2 but for 8–9 November 2004. The quiet day pattern is represented by the day 6 November 2004.

23:30 UT on 7 November, recovered to their normal values only after ~12:00 UT on 8 November. The magnetic activity continued with moderate intensity through the nights of 8–9 November during which the anomalous bubble zonal drift was observed, as to be discussed below. We may note that during the period of the bubble zonal drift analysis shown by shaded interval in Figure 6, B_z south condition with significant *AE* activity (~1500 nT) and small *Dst* decrease prevailed.

Figure 7 (top to bottom) shows the variations in the B_z (Figure 7a), *AE* (Figure 7b), the bubble zonal drift measured by all-sky imager over São João do Cariri

Similar to the event studied earlier, the westward reversal was registered at the same time also in the spread *F* irregularity zonal drift velocity as measured by the Digisonde at Fortaleza (Figure 7e). It is important to note that the vertical drift measured by the Digisonde (Figure 7d) that was downward near 23:00 UT (near the beginning of the decrease in the eastward zonal drifts in Figures 7c and 7e), started a steady decrease (with *AE* increasing) to turn to upward drift at about 22:15 LT. The V_z upward reversal appears to correspond to an *AE* intensification (under B_z south condition) that just preceded this feature. However, in view of the intense storm activity that prevailed for more than a day before these drift measurements, it is possible that some degree of disturbance dynamo electric field, accompanied by a disturbance thermospheric wind, must be playing a role in the drift variations observed on this night. ROCSAT-1 data analyzed by Fejer *et al.* [2008] showed that (in its seasonal average behavior for November) the DDEF polarity

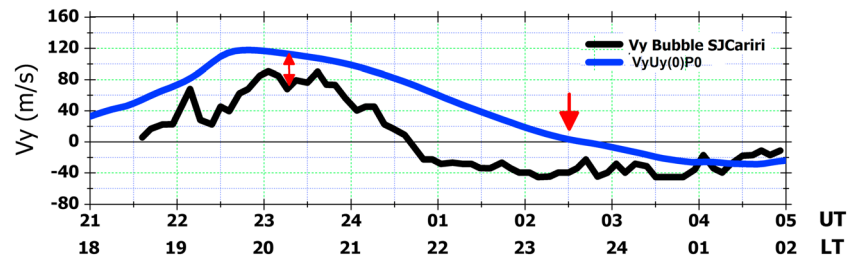


Figure 8. Calculated zonal plasma drift considering the original winds from HWM93 model (blue curve). The observed velocity of the plasma bubble is indicated by the black curve. The red arrows refer to some important points discussed in the text.

reversed to eastward at ~22:00 LT. Thus, it is likely that the disturbance dynamo electric field could be mainly responsible for the upward reversal of the vertical drift near 22:15 LT (in Figure 7), while the PPEF associated with the rapid increase of AE that occurred at this same time might have caused some modulations on the vertical drift. (It is important to note here that the upward drift reversal during this event occurred at an earlier local time, by about 1.5 h, than it did during the 23–24 September 2003 event of Figure 2). An accompanying disturbance zonal wind (expected to be westward) has probably modified the zonal drift that reversed westward at ~21:40 LT (00:40 UT) on this night. A little later in the sequence it is possible to observe that a rapid increase in the AE activity at 03:00 UT (00:00 LT), followed by its rapid fluctuations, produced a short duration downward V_z . This effect in the vertical drift appears to have been caused by an undershielding (and fluctuating) electric field but dominantly of westward polarity starting at this time (Figures 7b and 7d). The overall behavior of the drift variation on this night appears to follow the LT-dependent variations of disturbance electric field polarity as known from satellite measurements (as it was the case also on the nights of 23–24 September of the first event). For example, it is known from analysis of ROCSAT-1 data [Fejer *et al.*, 2008] that the polarity of the seasonally averaged PPEF (DDEF) can reverse from eastward (westward) to westward (eastward) around 22:00 LT in November. Some degree of day-to-day variability in this reversal time is to be expected however.

Similar to the previous event, the anticorrelation (indicated by the dotted blue lines) between zonal (V_{y_DE} , Figure 7e) and vertical (V_{z_DE} , Figure 7d) plasma drifts obtained by the Digisonde is evident in this case as well. The parameter $f_b E_s$ over FZ in Figure 7f showed a total absence of an E_s layer before 01:00 UT. (However, according to the discussion in section 3.1.2, it is reasonable to expect E_s layer occurrence at earlier hours at latitude northward of CP for which we do not have data to verify). From 01:00 UT, the AE index intensified and at this moment an E_s layer with a blanketing frequency around 1.5 MHz was created; however, in the following 2 h, this layer was interrupted and a layer was detected again from 03:50 UT.

3.2.1. Model Results

Initially the zonal drift was calculated considering the original winds according to the HWM93. The results for this case are presented in Figure 8. Similar to the September 2003 event, the calculated drift values (blue curve, identified by $V_y U_y(0)P0$) are higher than the observed drift (black curve). At ~23:15 UT, a difference of ~30 m/s can be noted between the two curves (as indicated by the red arrow). Additionally, the reversal of the plasma bubble drift to westward calculated using the zonal wind from the HWM93 occurred only at 02:30 UT, ~2 h after the time of the westward reversal of the observed drift.

Using the same methodology as that applied in the earlier event to the correction of the winds, but now multiplying the original zonal wind ($U_y(0)$) by a factor of 0.7, and using the same value of energetic particle precipitation (considering that this event could have the contribution from both the disturbance wind and the influences of an increase in the E region ionization), a more satisfactory result could be obtained, but a finer agreement between the observed and modeled drifts demanded a few more adjustments in the winds. Figure 9 presents the variations in the AE and the different control input parameters, with their modifications used for the zonal drift calculations, as well as the results of the drift under the different conditions. (The detailed description is identical to that of Figure 3). Figure 9f shown as blue curve (identified as $V_y U_y(i)P0$), the zonal drift obtained considering only the first order modified wind (by multiplying the HWM93 zonal wind by a factor of 0.7) (this latter identified in Figures 9c and 9d as $U_y(i)$). We note that this curve does not present a good agreement with the observed drift (black curve), especially regarding the time of the velocity reversal to westward that occurred ~2.5 h later than in the observational data. In Figure 9b, the ratio Σ_H/Σ_P represented by the blue curve was calculated using the low-latitude ionospheric model simulated by

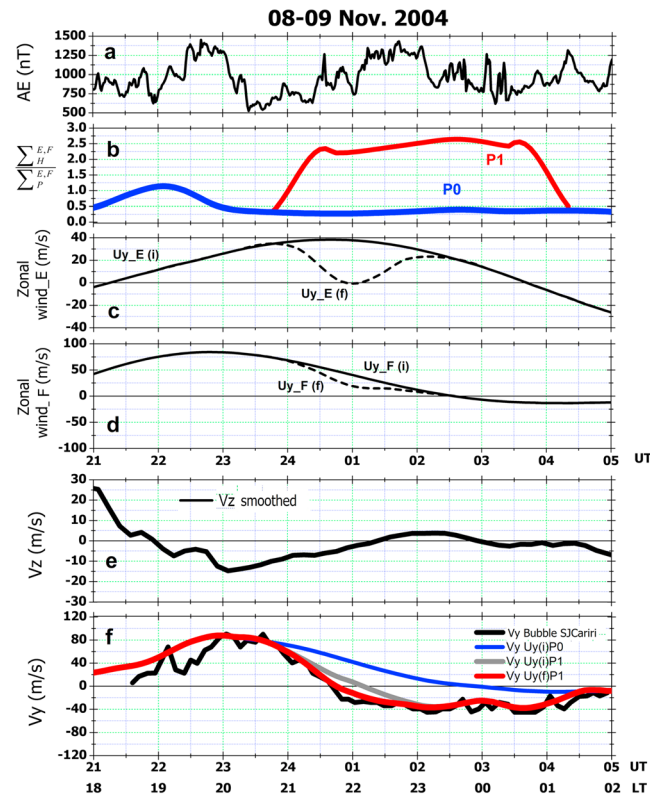


Figure 9. Similar to Figure 3 but during 8–9 November 2004.

to 2.5 in the ratio Σ_H/Σ_P (Figure 9b, red curve P1) was very important to improve the agreement of the calculated results with observed zonal drift, which is, especially, striking between 02:00 and 05:00 UT. However, a difference of ~30 min in the time of reversal can still be noted. Since the degree of magnetic activity during this event was very similar to that prevailed during the September 2003 (as mentioned earlier), we assumed that the precipitating particle energy spectrum could also be comparable for these two cases. On this basis, we opted to make a minor modification only in the zonal wind in order to obtain better agreement with the observed zonal drift. The modifications effected on the E and F-region zonal winds are shown as dotted curves (identified as $U_{y_E}(f)$ and $U_{y_F}(f)$) in Figures 9c and 9d. The new zonal drift result is represented by the red curve in Figure 9f, which demonstrates, during all the period evaluated, an almost perfect concordance with observed data. It is important to point out here that the modification in the zonal wind (by adding a westward disturbance component to the background wind) was a natural consequence of the fact that this episode was preceded by the severe storm of 8 November 2004, and it is known that enhanced westward wind perturbations can be present at equatorial latitude due to auroral heating associated with such severe storms [e.g., Sutton et al., 2005]. Besides this, the effect due to possible presence, in the wake of the severe storm, of a disturbance dynamo electric field whose polarity could turn eastward around 22:00 LT [Fejer et al., 2008] has been accounted for by the use of the Digisonde measured vertical drift (Figure 9e) in the calculation of the bubble zonal drift represented by the red curve in Figure 9f.

In summary, the results presented in Figure 9 show that both an increase in the ratio Σ_H/Σ_P as well as appropriate modifications in the zonal wind could play fundamental roles in the disturbance time plasma zonal drift variations and especially its nighttime reversal to westward at earlier local times than during quiet times. It is difficult to quantitatively isolate these two factors, in the absence of measurement of either/both of these parameters simultaneously with the drifts. However, one clear indication is that a more dominant role by energetic particle precipitation is possible when the westward drifts are observed under conditions of southward B_z and AE intensification as that occurred during both of these events. We may note further that although the zonal wind of the E region has been considerably modified around 00:40 UT (Figure 9c), it is found that the zonal drift is largely ruled by the zonal wind of the F region and the fact that this was not

the SUPIM-INPE (without including ionization by particle precipitation). This curve presents a small variation between 21:00 and 23:00 UT and a nearly constant value of 0.25 during the time interval in which the drift reversal was observed.

In order to achieve a better agreement with the observed behavior of the bubble westward reversal, we recalculated the zonal drift by including besides the modified neutral zonal wind, an increase in the ratio Σ_H/Σ_P generated by particle precipitation. As this event occurred under a similar condition as that of the event of September 2003, that is, over considerable influence of a magnetic activity (as seen in the AE variations) surrounding the bubble reversal time, we used the same energy spectrum for the precipitating electrons as that used for the first event in order to verify if it could produce the westward reversal of the drift as it did during the September 2003 event. The result for this analysis is shown by the gray curve in Figure 9f.

We can see that the increase from ~0.5

modified during 02:00 UT–04:30 UT when the calculated drift agreed perfectly with the observation would isolate the conductivity ratio as being solely responsible for maintaining the westward bubble drift, at least, during this period. *Abdu et al.* [2003] discussed a case of storm time westward bubble velocity when they suggested, based on qualitative considerations, that such drift was a result of combined effects of disturbance thermospheric winds and an increase in the *E* region ionization (Hall conductivity) possibly caused by energetic particle precipitation in the SAMA region.

3.2.2. Indications of the Ionization Enhancement in the *E* Region Recorded in the Ionograms

Figure 10 shows the ionograms from FZ on the night of 8–9 November 2004. We note the presence of strong spread *F* traces on this night. It was pointed out (earlier in section 3.1.2) that the *E* region ionization enhancement that is of concern here is that which is field line connected (mapped) to the equatorial *F* region (over Fortaleza in the present case) where the drift measurements are made. The latitude of the connected *E* region is located away (by about 10° from the equator), where we do not have any observations. The ionograms over FZ may serve as rough indicator, however. Three main characteristics can be identified that support the presence of enhanced night *E* region ionization. These are (1) the tendency of trace curvature at the lower frequency end of the *F* layer trace. This characteristic is indicative of group delay due to ionization at *E* layer heights, such as that marked by the black circle in the ionogram at 00:20 UT but also apparent in the ionograms (for example, at 01:00 UT) around the time at which the reversal of the plasma bubble occurred; (2) the formation of an *Es* layer during the interval in which the bubble was constantly moving to west. Initially an *Es* layer was detected at 01:00 UT at ~110 km; however, the ionograms show that this layer weakens and is completely interrupted at 01:30 UT. After this, the next ionograms showed a total absence of any *Es* layer, but from 03:30 UT, a new layer is formed which clearly presented range spreading feature very common in *Es* layer formed by energetic particle precipitation [see *Abdu et al.*, 2013] as discussed before. It is possible to verify that this layer blocks the lower frequency end of *F* layer trace in the ionogram at 04:10 UT (the $f_b E_s$ being 2.5 MHz); (3) anomalous *Es* formation at ~130 km between 06:00 and 06:50 UT presenting varying degrees of range spreading can be noted which was similar to that observed during the storm of September 2003 and other events studied by *Santos et al.* [2016]. The *Es* layers presenting range spreading can be associated with precipitation of energetic particle in the SAMA as discussed before. Additionally, there is a considerable decrease in the critical frequency of the *F* layer (as can be verified in the ionograms between the two vertical blue arrows). The $f_o F_2$ parameter decreased from 11 MHz at 01:50 UT, to 5.5 MHz at 06:50 UT. It is interesting to note that it was during this interval of decrease in $f_o F_2$ that the sporadic *Es* layer was formed and intensified. A decrease in $f_o F_2$ is indicative of a decrease in the field line-integrated Pedersen conductivity and therefore of enhancement in the ratio Σ_H/Σ_P , which can favor the *Es* layering process.

Figure 11 shows the ionograms over São José dos Campos (SJC) (23.2°S, 45.9° W), near Cachoeira Paulista and closer to the center of the SAMA, that are representatives of the times in which the bubble presented a decrease in its eastward velocity (near 23:30 UT) until the moment of the total reversal of the drift to west. During the interval that the bubble was reversing to west, the *Es* layer trace presented a certain degree of range spreading and increase of $fbEs$ (as can be noted in the ionograms shown during 23:30 UT and 00:50 UT), which indicated enhanced *E* layer ionization, thus providing evidence of energetic particle precipitation during the reversal and the continuing westward drift of the plasma bubbles and the associated irregularities. In addition, we can verify that very near to the time of the bubble zonal drift reversal, the *Es* layer at 00:35 UT suffer an intensification in relation to its intensity in the previous ionogram. The tendency of trace curvature at the lower frequency end of the *F* layer trace, which is also an indication of the *E* region ionization enhancement, can be noted in the ionograms at 00:10 UT and 00:20 UT. The increase in the Σ_H/Σ_P in this case is caused mainly by enhancement in Σ_H due to particle ionization in the *E* region rather than due to a possible decrease of Σ_P arising from a decrease in $f_o F_2$.

4. Final Remarks

The zonal drift of the spread *F* plasma bubbles and associated smaller-scale irregularities were investigated here using data collected by an all-sky imager at São João do Cariri and Digisondes at Fortaleza and Cachoeira Paulista during two events of magnetic storms. The eastward drift velocities of the bubbles on the nights of these disturbances were significantly smaller than their quiet time values. Further, during both the events studied, excellent agreement was found between the zonal drift pattern obtained from the imager

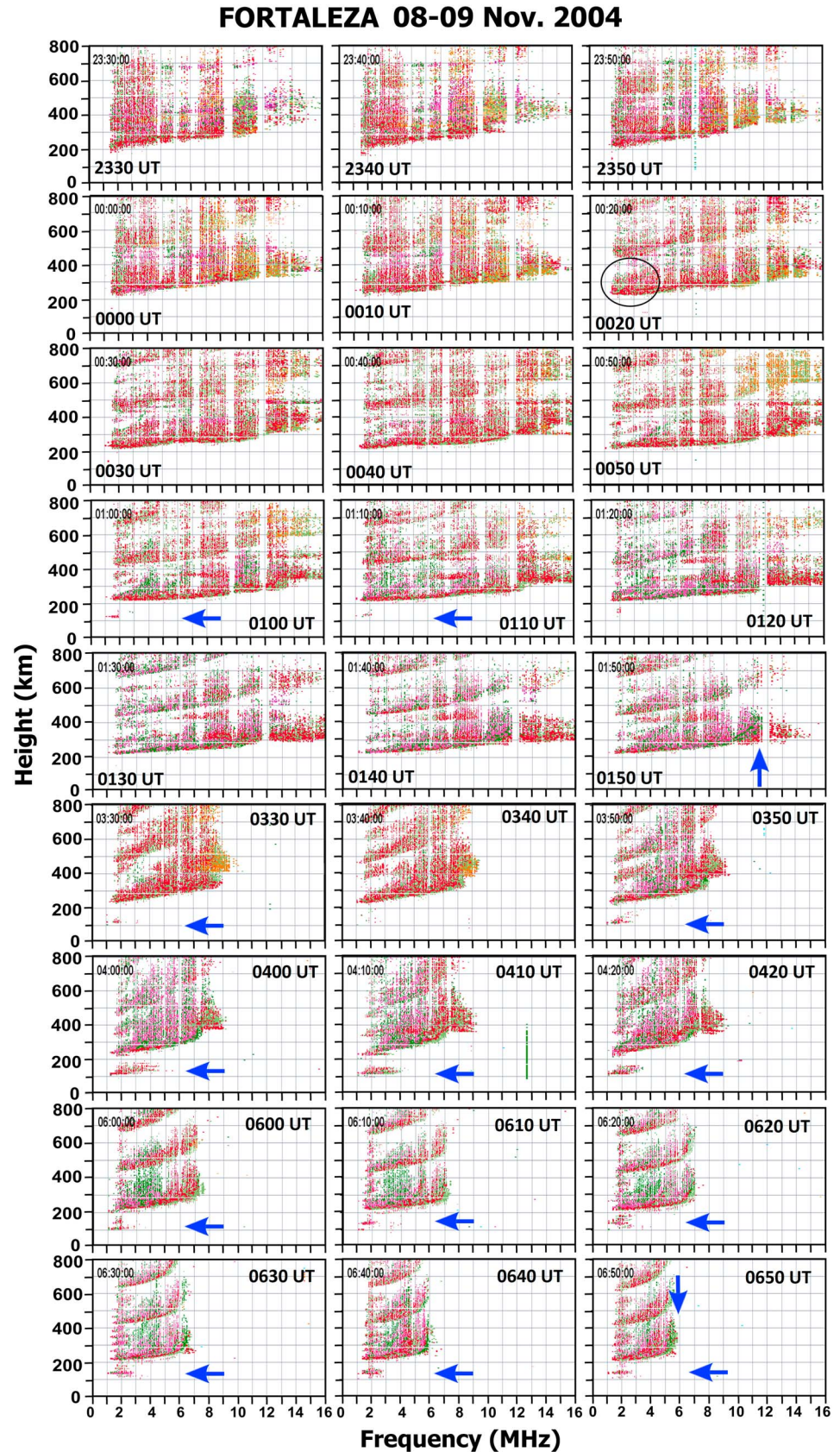


Figure 10. Similar to Figure 5 but for 8–9 November 2004. The vertical arrows highlight the decrease in the f_oF_2 parameter.

São José dos Campos - 08 Nov. 2004

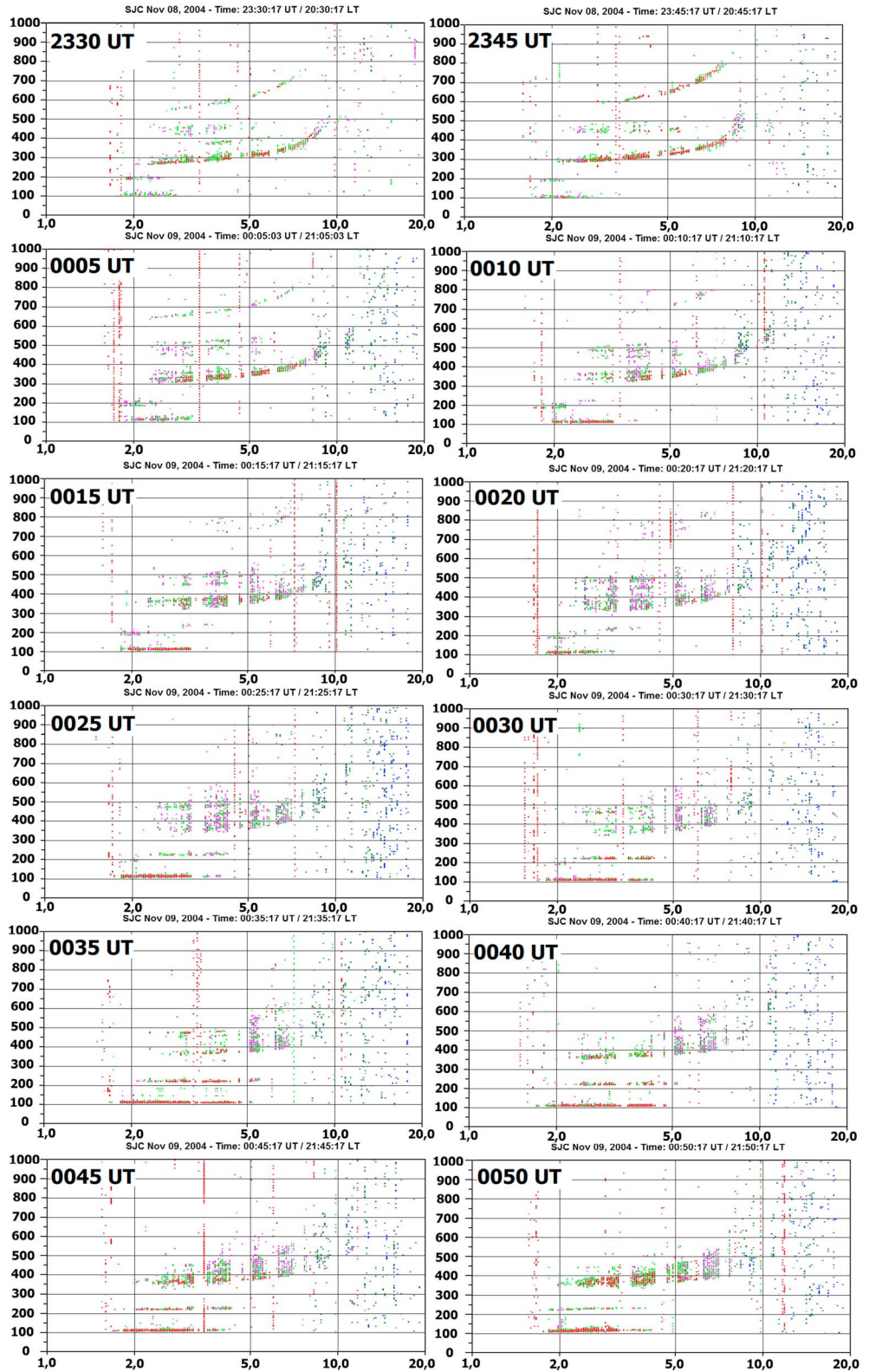


Figure 11. Ionograms from São José dos Campos for 8 November 2004. The x axis corresponds to frequency (MHz) and the y axis corresponds to height (km).

and that measured by the Digisonde, with respect to their westward reversal that occurred during an intensification of the magnetic activity (in *AE*). Further, the variations in the zonal drift and vertical drift (measured by the Digisonde) were found to be anticorrelated.

In an attempt to explain the electrodynamics of the observed drift variations, we modeled them using a low-latitude ionosphere simulated by the SUPIM-INPE and considering the contributions arising from field line integrated quantities of the conductivity weighted winds and the Hall-to-Pedersen conductivity ratio. The relative contributions from the wind and the conductivity ratio were adjusted based on the degree of the disturbances. The initial values of the zonal wind as adopted from the HWM93 was modified when necessary using a reference the well established zonal drift characteristics over Jicamarca. The field line-integrated conductivity ratio was adjusted in the light of the prevailing magnetic activity and the consideration that associated energetic particle precipitation in the ionosphere can occur under the influence of the SAMA.

In the case of the September 2003 storm event, the calculated initial zonal drift was found to be very different from the observed drift. Based on the zonal drift variation over Jicamarca as reference the possibility appeared clear that the wind model used in the calculations of the zonal drift was inappropriate. After adequate adjustments in the zonal wind, substantial improvements were achieved in the calculated zonal drift, but a delay of ~ 3.5 h in the time of westward reversal (in the postmidnight hours) of the bubble drift was still present. The drift reversal occurred under significant influence of magnetic disturbance, (as indicated by the prevailing *AE* activity), when it is known that, besides the penetration electric field, enhanced energetic particle precipitation can influence the electrodynamic of the ionosphere over the SAMA region. Inclusion of this effect in the calculations by suitably increasing the ratio of field line-integrated conductivities resulted in excellent agreement between the calculated drift and the observation during the period of its westward reversal. Thus, the results obtained in this work show that the modification of the reference zonal wind was a fundamental constraint for a satisfactory representation of zonal drift, especially in its eastward phase, but the reversal of the bubble to west and the maintenance of the westward velocity could only be simulated when the effects of the energetic particle precipitation, through an increase in the ratio Σ_H/Σ_P were taken into account, thereby demonstrating the dominant role of a vertical Hall electric field in driving the westward reversal of the bubble zonal drift.

Analysis of the ionograms during this magnetic storm showed anomalous occurrences of sporadic *E* layers over FZ, preceded by their occurrence over CP. These *E_s* layers presented characteristics such as range spreading of echoes and blanketing of *F* layer traces, indicative of enhanced ionization in the *E* layer due to energetic particle precipitation that contributed to enhanced ratio of Σ_H/Σ_P . The occurrence time of these layers was coincident with the interval that the bubble zonal drift reversed and remained westward. This result reinforced the idea that the peculiarities observed in the dynamics of the plasma bubble could have strong influence from the effects generated by the energetic particle precipitation in the presence of a prompt penetration electric field besides a possibly more direct influence from a storm associated a disturbance zonal wind, which however, appeared to be insignificant in this episode.

Regarding the event of November 2004, similar adjustments were made in order to simulate the plasma bubble zonal drift variation as a whole and its westward reversal in particular. Adjustments were made in both the zonal wind as well as in the field line-integrated conductivity ratio using similar criteria as was used in the case of the September 2003 event. Additionally it was found necessary to include a disturbance westward wind in the approach to obtain better agreement between the calculated and observed bubble drift reversal to westward (near 22:00 LT). In this case, the variations in f_oF_2 and the *E_s* layer parameters in the ionograms over FZ suggested that the increase in the ratio Σ_H/Σ_P required to bring about agreement between the calculated zonal drift reversal to westward and the observed features could be the result of both an increase in Σ_H (identified by the *E_s* layer presence) as also a decrease in Σ_P (identified by a decrease in f_oF_2 parameter). It was verified that over São José dos Campos, a location close to the center of the SAMA (like CP), the increase of the sporadic *E* layer activity was more dominant than a decrease in f_oF_2 during the drift reversal to westward. Thus, the results from the analysis of this storm demonstrate that a vertical Hall electric field induced by a primary zonal prompt penetration electric field in the presence of enhanced ionization (conductivity) in the nighttime *E* region together with a disturbance westward wind can cause westward reversal of the equatorial plasma bubble drifts from their normally eastward direction. During both the storms, it was noted that the eastward zonal drift that prevailed before reversal to westward was significantly smaller than its average

quiet time values. The zonal drift velocity at its peak around 20:00–21:00 LT was on the order of 80 m/s in both cases, whereas their quiet time values are usually in the range of 120–130 m/s. This significant decrease in the eastward drift might perhaps be considered as an indicator that any disturbance zonal wind known to be originating from auroral heating acquiring westward momentum due to Coriolis effect, if present, must be acting against the normal eastward wind in the equatorial region [see for example, Emmert *et al.*, 2002; Sutton *et al.*, 2005], and in the case of the event 2 (under the influence of a more intense storm), additional perturbation westward wind appears to have contributed to the precise timing of the westward drift reversal.

The *Es* layers with peculiar characteristics of range spreading echoes and significant blanketing frequency have been shown to be evidence of storm time energetic particle precipitation [Abdu *et al.*, 2013]. The formation of such *Es* layers through ion convergence process by vertical Hall electric field was shown to be operative in the height region near 100 km, its efficiency decreasing rapidly with increase in altitude. In the results presented here such layer was indeed observed, but additionally, as in case of 24 September 2003 over FZ, it became more intense toward the end in a sequence of descending type *Es* layer, which is known to indicate the descending null point of a tidal mode wind shear. Formation of nondescending type *Es* layer near 130 km was also observed (as in the case of 9 November 2004). In any case the competing/complementary roles played by the wind shear mechanism, ionization by energetic particle precipitation, and instability process producing plasma structuring (to cause range spreading echoes) in the formation of these *Es* layers are not sufficiently well understood. Our future work will focus on gaining a better understanding of such *Es* layer processes vis-à-vis storm time equatorial plasma bubble dynamics.

Acknowledgments

5A.M. Santos would like to acknowledge the Conselho Nacional de Desenvolvimento Científico e Tecnológico-CNPq for the financial support under grants 150403/2015 and 160088/2011-9, and PNPd/CAPES Space Geophysics Program at INPE. C.M. Denardini thanks CNPq/MCTI (grant 303121/2014-9), FAPESP (grant 2012/08445-9). The authors thank DAE/INPE for kindly providing the Digisonde and 630 nm all-sky imager data. The Digisonde data used in this study may be acquired by contacting the Responsible Coordinators in DAE/INPE (Inez S. Batista, e-mail: inez.batista@inpe.br). The authors thank the Embrace/INPE Program for kindly providing the magnetic data (<http://www.inpe.br/spaceweather>). The SYM-H, AE, and IMF data were obtained from the website http://omniweb.gsfc.nasa.gov/form/omni_min.html. M.A. Abdu acknowledges the support received from the Coordenação de Aperfeiçoamento de Pessoal de Nível Superior (Capes) for a senior visiting professorship at ITA/DCTA. The authors are grateful to M. T. A. H. Muella and P. R. Fagundes (Laboratory of Physics and Astronomy at Institute of Research and Development-University of Vale do Paraíba (UNIVAP)) for providing the ionosonde data from São José dos Campos.

References

- Abdu, M. A., P. T. Jayachandran, J. MacDougall, J. F. Cecile, and J. H. A. Sobral (1998), Equatorial *F* zonal plasma irregularity drifts under magnetospheric disturbances, *Geophys. Res. Lett.*, *25*, 4137–4140, doi:10.1029/1998GL900117.
- Abdu, M. A., I. S. Batista, H. Takahashi, J. MacDougall, J. H. Sobral, A. F. Medeiros, and N. B. Trivedi (2003), Magnetospheric disturbance induced equatorial plasma bubble development and dynamics: A case study in Brazilian sector, *J. Geophys. Res.*, *108*(A12), 1449, doi:10.1029/2002JA009721.
- Abdu, M. A., I. S. Batista, A. J. Carrasco, and C. G. M. Brum (2005), South Atlantic magnetic anomaly ionization: A review and a new focus on electrodynamic effects in the equatorial ionosphere, *J. Atmos. Sol. Terr. Phys.*, *67*, 1643–1657.
- Abdu, M. A., E. A. Kherani, I. S. Batista, and J. H. A. Sobral (2009), Equatorial evening prereversal vertical drift and spread *F* suppression by disturbance penetration electric fields, *Geophys. Res. Lett.*, *36*, L19103, doi:10.1029/2009GL039919.
- Abdu, M. A., I. S. Batista, F. Bertoni, B. W. Reinisch, E. A. Kherani, and J. H. A. Sobral (2012), Equatorial ionosphere responses to two magnetic storms of moderate intensity from conjugate point observations in Brazil, *J. Geophys. Res.*, *117*, A05321, doi:10.1029/2011JA017174.
- Abdu, M. A., J. R. Souza, I. S. Batista, B. G. Fejer, and J. H. A. Sobral (2013), Sporadic *E* layer development and disruption at low latitudes by prompt penetration electric fields during magnetic storms, *J. Geophys. Res. Space Physics*, *118*, 2639–2647, doi:10.1002/jgra.50271.
- Anderson, D., A. Anghel, K. Yumoto, M. Ishitsuka, and E. Kudeki (2002), Estimating daytime vertical $E \times B$ drift velocities in the equatorial *F* region using ground-based magnetometer observations, *Geophys. Res. Lett.*, *29*(12), 1596, doi:10.1029/2001GL014562.
- Basu, S., S. Basu, E. MacKenzie, C. Bridgwood, C. E. Valladares, K. M. Groves, and C. Carrano (2010), Specification of the occurrence of equatorial ionospheric scintillations during the main phase of large magnetic storms within solar cycle 23, *Radio Sci.*, *45*, R55009, doi:10.1029/2009RS004343.
- Blanc, M., and A. D. Richmond (1980), The ionospheric disturbance dynamo, *J. Geophys. Res.*, *85*, 1669, doi:10.1029/JA085A04p01669.
- Emmert, J. T., B. G. Fejer, G. G. Shepherd, and B. H. Solheim (2002), Altitude dependence of middle and low-latitude daytime thermospheric disturbance winds measured by WINDII, *J. Geophys. Res.*, *107*(A12), 1483, doi:10.1029/2002JA009646.
- Fejer, B. G., and J. T. Emmert (2003), Low-latitude ionospheric disturbance electric field effects during the recovery phase of the 19–21 October 1998 magnetic storm, *J. Geophys. Res.*, *108*(A12), 1454, doi:10.1029/2003JA010190.
- Fejer, B. G., J. W. Jensen, and S. Y. Su (2008), Seasonal and longitudinal dependence of equatorial disturbance vertical plasma drifts, *Geophys. Res. Lett.*, *35*, L20106, doi:10.1029/2008GL035584.
- Huang, C. S., S. Sazykin, J. L. Chau, N. Maruyamad, and M. C. Kelley (2007), Penetration electric fields: Efficiency and characteristic time scale, *J. Atmos. Sol. Terr. Phys.*, *69*, 1135–1146, doi:10.1016/j.jastp.2006.08.016.
- Huang, C.-S., and P. A. Roddy (2016), Effects of solar and geomagnetic activities on the zonal drift of equatorial plasma bubbles, *Geophys. Res. Space Physics*, *121*, 628–637, doi:10.1002/2015JA021900.
- Kouba, D., J. Boska, I. A. Galkin, O. Santolik, and P. Sauli (2008), Ionospheric drift measurements: Skymap points selection, *Radio Sci.*, *43*, R51590, doi:10.1029/2007RS003633.
- Kozlov, A., and V. V. Pazmukhov (2008), Digisonde drift analysis software, in radio sounding and plasma physics, *AIP Conf. Proc.*, *974*, 167–174, doi:10.1063/1.2885026.
- Li, G., B. Ning, B. Zhao, L. Liu, W. Wan, F. Ding, J. S. Xu, J. Y. Liu, and K. Yumoto (2009), Characterizing the 10 November 2004 storm time middle-latitude plasma bubble event in Southeast Asia using multiinstrument observations, *J. Geophys. Res.*, *114*, A07304, doi:10.1029/2009JA014057.
- Mathews, J. D. (1998), Sporadic E: Current views and recent progress, *J. Atmos. Sol. Terr. Phys.*, *60*(4), 413–435, doi:10.1016/S1364-6826(97)00043-6.
- Reinisch, B. W., J. L. Scali, and D. M. Haines (1998), Ionospheric drift measurements with ionosondes, *Ann. Geofis.*, *41*(N. 5-6), 695–702, doi:10.4401/ag-3812.
- Richmond, A. D., C. Peymirat, and R. G. Roble (2003), Long-lasting disturbances in the equatorial ionospheric electric field simulated with a coupled magnetosphere-ionosphere-thermosphere model, *J. Geophys. Res.*, *108*(A3), 1118, doi:10.1029/2002JA009758.

- Santos, A. M., M. A. Abdu, J. R. Souza, J. H. A. Sobral, and I. S. Batista (2016), Disturbance zonal and vertical plasma drifts in the Peruvian sector during solar minimum phases, *J. Geophys. Res. Space Physics*, *121*, 2503–2521, doi:10.1002/2015JA022146.
- Sobral, J. H. A., et al. (2006), Equatorial ionospheric responses to high-intensity long-duration auroral electrojet activity (HILDCAA), *J. Geophys. Res.*, *111*, 07502, doi:10.1029/2005JA011393.
- Sobral, J. H. A., et al. (2009), Ionospheric zonal velocities at conjugate points over Brazil during the COPEX campaign: Experimental observations and theoretical validations, *J. Geophys. Res.*, *114*, A04309, doi:10.1029/2008JA013896.
- Sobral, J. H. A., et al. (2011), Midnight reversal of ionospheric plasma bubble eastward velocity to westward velocity during geomagnetically quiettime: Climatology and its model validation. *J. Atmos. Sol. Terr. Phys.*, *73*, 1520–1528, doi:10.1016/j.jastp.2010.11.031.
- Sutton, E. K., J. M. Forbes, and R. S. Nerem (2005), Global thermospheric neutral density and wind response to the severe 2003 geomagnetic storms from CHAMP accelerometer data, *J. Geophys. Res.*, *110*, A09S40, doi:10.1029/2004JA010985.
- Tsurutani, B. T., and W. D. Gonzalez (1987), The cause of high-intensity long-duration continuous AE activity (HILDCAAs): Interplanetary Alfvén wave trains, *Planet. Space Sci.*, *35*, 405–412.
- Valentim, A. M. S. (2015), Campos elétricos e derivas do plasma na ionosfera equatorial do setor americano durante tempestades magnéticas, PhD thesis, 256 pp., National Institute for Space Research, São José dos Campos, São Paulo, Brazil, 15 April.
- Whitehead, J. (1970), Production and prediction of sporadic E, *Rev. Geophys. Space Phys.*, *8*(1), 80, doi:10.1029/RG008i001p00065.